Crack-Free Silicon Monoxide as Anode for Lithium Ion Battery

AUTHOR NAMES

Wenquan Lu[1,], Xinwei Zhou[2,3], Yuzi Liu[2], and Likun Zhu[3]*

AUTHOR ADDRESS

1. Chemical Sciences and Engineering, Argonne National Laboratory, Lemont IL 60439
2. Center for Nanomaterials, Argonne National Laboratory, Lemont, IL 60439
3. Department of Mechanical and Energy Engineering, Indiana University Purdue University Indianapolis, Indianapolis, IN 46202

AUTHOR INFORMATION

[*]**Corresponding author**: luw@anl.gov

Key words: silicon monoxide, silicon, microstructure, isotropic expansion, single particle battery, lithium ion battery

---

This is the author's manuscript of the article published in final edited form as:

Lu, W., Zhou, X., Liu, Y., & Zhu, L. (2020). Crack-Free Silicon Monoxide as Anodes for Lithium-Ion Batteries. ACS Applied Materials & Interfaces, 12(51), 57141–57145. https://doi.org/10.1021/acsami.0c18321

ABSTRACT

The volume expansion of Si and SiO particles was investigated using single particle battery assembled with focused ion beam and scanning electron microscopy (FIB-SEM) system. Single Si and SiO particles were galvanostatically charged and discharged as in real batteries. Microstructure changes the particles were monitored in in-situ condition using FIB-SEM from two different angles. The results reveal that the volume expansion of micrometer size particle SiO is not only much smaller than that of Si, but also kept its original shape with no sign of cracks. This isotropic mechanical property of SiO particle can be attributed to its microstructure: nano size Si domains mixed with SiO_2 domains. The nano size Si domains can mitigate the anisotropic swelling caused by the orientation-dependent lithium ion insertion; The surrounding SiO_2 domains can act as a buffer to further constrain the localized anisotropic swelling.

TOC GRAPHICS

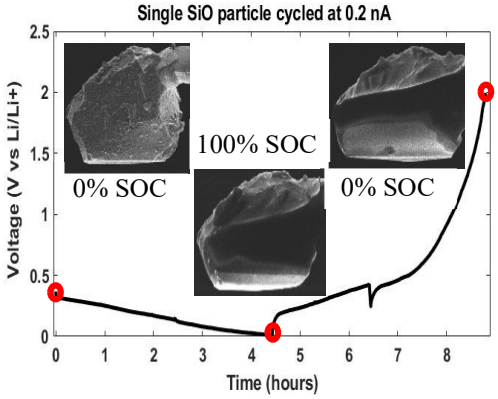

INTRODUCTION

Due to its exceptional high capacity, Si has been viewed as a next generation anode material to improve the energy density of lithium ion batteries (LIB) [1-7]. However, insurmountable issues, such as large volume expansion and high reactivity of lithiated Si with electrolyte, keep Si as a long shot to be commercialized, despite the relentless efforts and progress made in the past decade [3, 8-10]. After many years' studies, we believe that the alternative anode material, micrometer size silicon monoxide (SiO), could provide a promising solution due to its large specific capacity, ease of handing, and less volume expansion compared to nano size Si particles[11-18].

Though written as SiO, silicon monoxide is not a pure compound, instead, it consists of Si and SiO_2 nano-domains (Si-SiO_2 composite) [12, 19]. Si nano-domain, the electrochemical active component, has size in nanometers, which itself is small enough to withhold the stress caused by volume expansion/contraction during lithiation and delithiation [1, 6]. The surrounding SiO_2 domain is expected to provide further constraint to the Si domain. Another beneficial effect of the SiO_2 domain around Si domain is to allow less contact area between Si and electrolyte, leading to less lithium-consuming SEI formation reactions. Even so, SiO can still expand by up to 160%[20], which makes a better understanding of the volume and possible morphology changes of SiO particle very important to enable the optimized electrode design and good electrochemical performance.

Recently single particle battery (SPB), couple with focused ion beam-scanning electron microscopy (FIB-SEM), was developed for in-situ and operando observation of the dynamic

morphology changes of Sn, Ge, and P [21-24]. A similar experiment was conducted on SiO to investigate its microstructural changes during charge and discharge; while a Si particle was used as control. The experiment was performed on a Zeiss Nvision 40 FIB-SEM at the Center for Nanoscale Materials, Argonne National Laboratory.

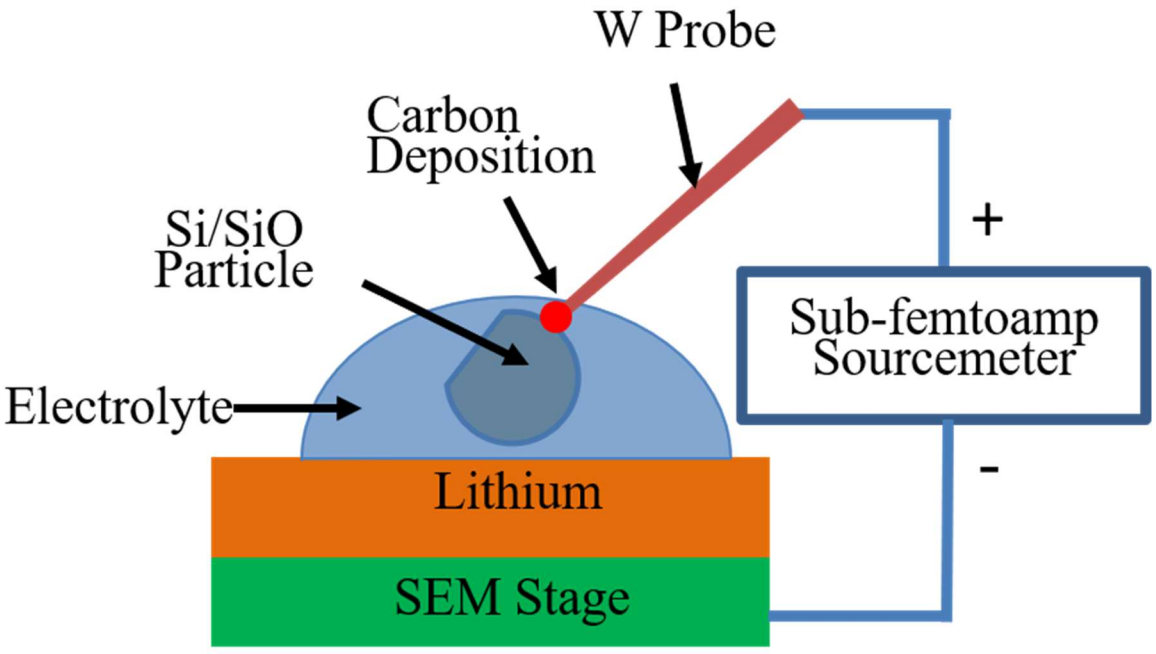

Figure 1. Schematic diagram of single particle battery in SEM: Si/SiO particle "weld" on tungsten probe acting as the working electrode; lithium metal acting as the counter electrode to provide lithium ions; electrolyte is prepared by dissolving LiTFSI in a solvent of 1-butyl-1-methylpyrrolidinium bis (trifluoromethylsulfonyl) imide (P_{14}TFSI) ionic liquid; a Sub-femtoamp source meter is used to electrochemically charge and discharge the particle.

MATERIALS AND METHODS

Structure of Si and SiO: The 99.9% pure Si and SiO were purchased from American Element (USA) and Osaka Titanium Tech. (Japan), respectively. High-Energy X-Ray Diffraction (HE-XRD) experiments were performed at the beamline 11-ID-C of the Advanced Photon Source at Argonne National Laboratory (ANL). The X-ray wavelength is 0.1173 Å and a PerkinElmer 2D area detector was used to collect 2D XRD patterns. Transmission electron microscopy (TEM) measurements were taken using a JEM-2100F field emission TEM (JEOL, Peabody, Mass.) at Center for Nanoscale Materials (CNM) at ANL.

Fabrication of single particle battery (SPB): The experiment was performed on a Zeiss Nvision 40 FIB-SEM at the Center for Nanoscale Materials, Argonne National Laboratory. The single particle battery (SPB) diagram can be seen in **Figure 1** and the detailed information can be found in the literature.[21] To build SPB, the particle electrode was first fabricated by attaching one particle to the tungsten probe using ion beam carbon deposition. The Li metal was placed on top of the SEM stub as the counter electrode. One drop of ionic liquid electrolyte (ILE) was placed on top of Li metal. The ILE consists of lithium bis (trifluoromethylsulfonyl) imide (LiTFSI) salt (Sigma-Aldrich) and 1-butyl-1 methylpyrrolidinium bis (trifluoromethylsulfonyl) imide(P_{14}TFSI) solvent (Sigma-Aldrich). The vapor pressure of P_{14}TFSI is close to zero, which makes this liquid suitable for the vacuum environment in FIB-SEM.[21]

Electrochemical lithiation and dilithiation: The SPB cycling was controlled by a Keithley 6430 sub-femtoamp remote source meter from Tektronix. Similar to the charge/discharge of a real LIB, constant current (galvanostatic mode) was used to lithiate and delithiate the Si or SiO single particle battery. The theoretical capacity of the single particle was estimated from the size of Si or SiO particles.

FIB-SEM imaging: The particle was lifted out from the ILE for imaging at different states of lithiation. In order to visualize the microstructure change of the particle, the imaging area was polished by FIB to remove ILE on the surface to expose the cross section of the particle. Typically, only a few nanometers in depth of the particle is removed during the polishing process to mitigate the particle morphology changes. The front view (perpendicular to cross section) and top view (parallel to the cross section) of the particle were taken using the both scanning electron microscope (SEM) and FIB, respectively. The electron beam and ion beam remain closed other than for taking images.

RESULTS AND DISCUSSION

As shown in **Figure 2a,** three major sharp peaks of Si XRD pattern at $2\theta = 2.14, 3.50, 4.10$ correspond to the characteristic crystal peaks of Si and support a good crystalline structure of the sample. The crystallinity is confirmed by the TEM image in **Figure 2b,** which displays the Si (111) lattice, marked by parallel red lines, with an interplanar spacing of 3.1 Å. However, no sharp peak is observed on XRD pattern of SiO in **Figure 2a**. Three broad peaks at SiO observed at $2\theta = 1.73, 3.78$, and 5.52 can be attributed to SiO_x. A couple of shoulder peaks at around $2\theta = 2.14$ and 3.50 can be attributed to Si. The less intensity of these two peaks and broadening feature indicate the amorphous feature of local Si in SiO particles. HRTEM image of SiO particle in **Figure 2c** confirms that there are indeed nanosized crystalline domains within an amorphous matrix, though the boundary of the silicon crystalline domains is not very clear and well defined. Calculating from the HRTEM image, the lattice constant for some crystalline nanodomains is 3.1 Å, characteristic of Si bulk.

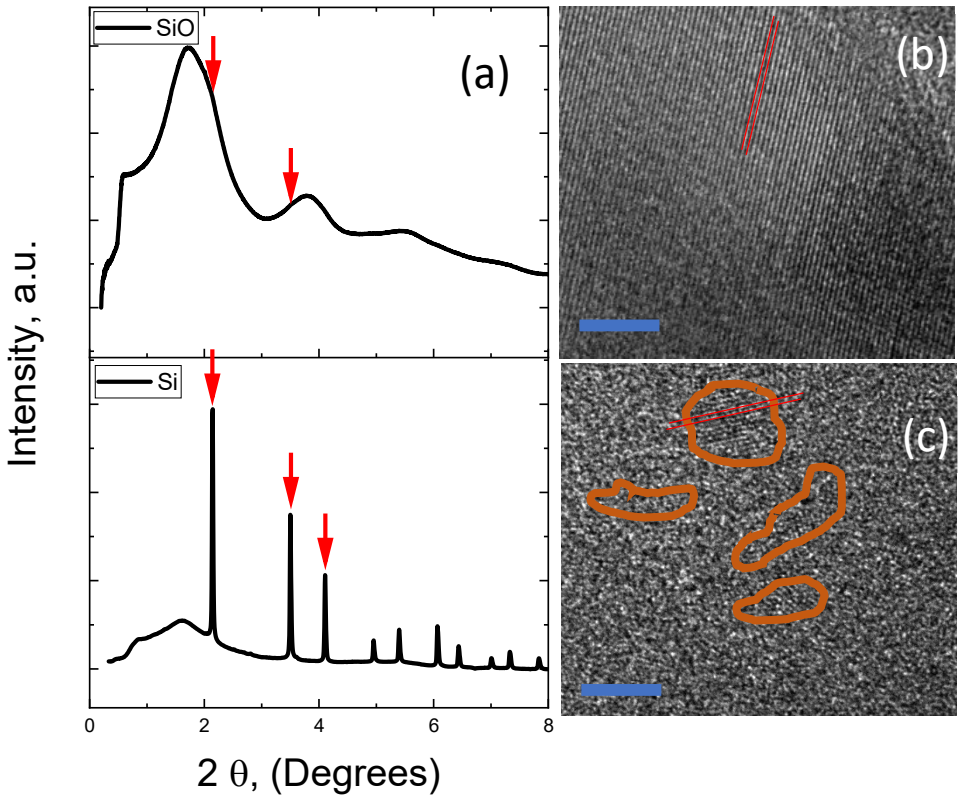

Figure 2. (a) XRD pattern of Si and SiO. TEM images of (b) Si, and (c) SiO. The scale bar in (b) and (c) is 5 nm.

Before lithiation, the pristine Si particle appears with regular shape and distinct edges as shown in the SEM and FIB images, **Figure 3a** and **Figure 3e**, from two different viewing angles (front view and top view). The front and top surfaces of the Si particle are very flat and smooth. The volume of the Si particle is estimated to be 144 μm^3. The capacity of this single Si particle is calculated to be 1.2 nAh, assuming 3710 mAh/g capacity of Si. Then, 0.1 nA (~ C/10 rate) was applied to the SPB for lithiation and delithiation between 5 mV and 1.5 V. The total lithiation and delithiation time from **Figure 3h** are about 12.8 and 11.4 hours, respectively, which are very

close to the capacity estimation. It can also be seen from Figure 2h that the voltage profile of the Si-SPB is the same as the conventional composite Si electrode, with flat voltage around 0.06 V during lithiation and around 0.40 V during delithiation. We then have confidence to believe that the change of the single Si particle in SPB represents the change of Si particles in the composite electrode.

The fully lithiated Si particle was lifted off the ILE for SEM and FIB imaging. The front and top views of the Si particle, shown in **Figure 3b** and **Figure 3f**, indicate that the particle greatly expanded and completely lost its original shape. The irregular shape of the fully lithiated Si particle suggests that the lithiation process for this Si particle was not isotropic. **Figure 3c** and **Figure 3g** show that the fully delithiated Si particle shrunk a lot, but, not back to its original shape, which suggests irreversible morphology changes of Si during its lithiation and delithiation processes.

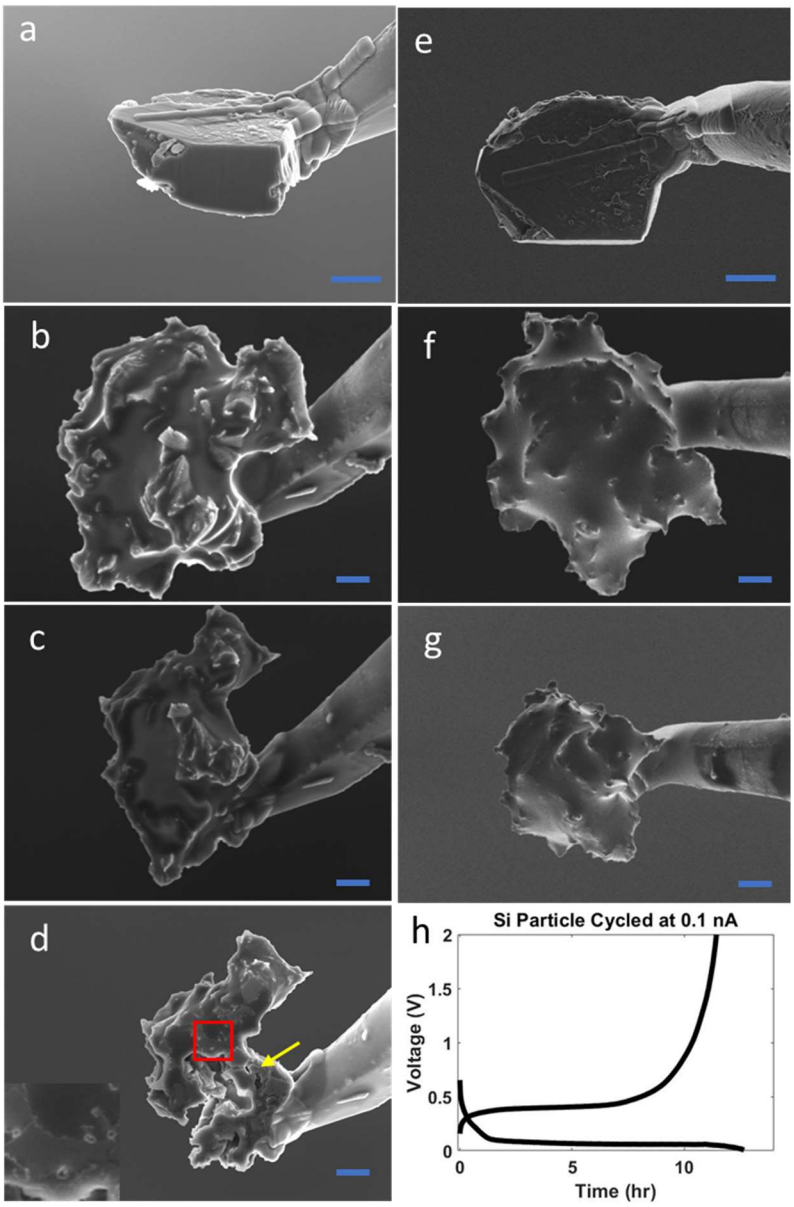

Figure 3 Front and top views of Si particle were taken by SEM (left column) and FIB (right column), respectively, at various states of lithiation: (a/e) before lithiation, (b/f) after full lithiation, (c/g) after full delithiation, and (d) cross section of fully delithiated Si, (h) voltage profile of lithiation and delithiation with constant current at 0.1 nA. The scale bar in this SEM images is 2 μm.

The front side of the fully delithiated Si particle was repeatedly polished to expose its inside microstructure. The evolution of the microstructural change of the delithiated Si is shown in supporting movie-Si. A representative image, shown in **Figure 3d**, reveals pores and cracks (see the arrows and enlarged part of red square area at the bottom left corner of this figure) in the delithiated particle. The cracks are caused by the particle expansion and contraction during the lithiation and delithiation processes. The formation of pores may be caused by a different mechanism: the vacancy-mediated diffusion during the delithiation process, analogous to a Sn particle[21, 22]. Though cracks and pores were observed during the 1st lithiation and delithiation, around 90% Coulombic efficiency was obtained, suggesting that the particle has a continuous connection between cracks. We can expect that the particle will pulverize completely and lose capacity with more cycles.

A similar FIB-SEM experiment was conducted on SiO particle in SPB. The front and top views from SEM and FIB images of pristine SiO are shown in **Figure 4a** and **Figure 4e**. The SiO pristine particle has a relatively round shape with a smooth surface. The front side was polished using the FIB before taking images. The polishing depth was about 5 nm, which is deep enough to observe the fresh inside of SiO particle without changing the overall particle morphology. The clean-cut line can be seen from the sharp line at the bottom of the FIB image. This polishing step was conducted each time before taking SEM/FIB images at the end of the lithiation and delithiation, respectively.

The volume of the SiO particle is estimated to be 288 μm^3. The capacity of this single SiO particle is calculated to be 1.0 nAh, assuming 1710 mAh/g capacity of SiO. Then, 0.2 nA (~ C/5 rate) was applied to the SPB for lithiation and delithiation between 5 mV and 1.5 V. The total lithiation and delithiation times from **Figure 4h** are about 4.5 hours, which are very close to the

capacity estimation. It can also be seen from Figure 4h that the voltage profile of the SiO-SPB is the same as the conventional composite SiO electrode. The downward spike in the middle of the delithiation process is due to the current interruption for imaging.

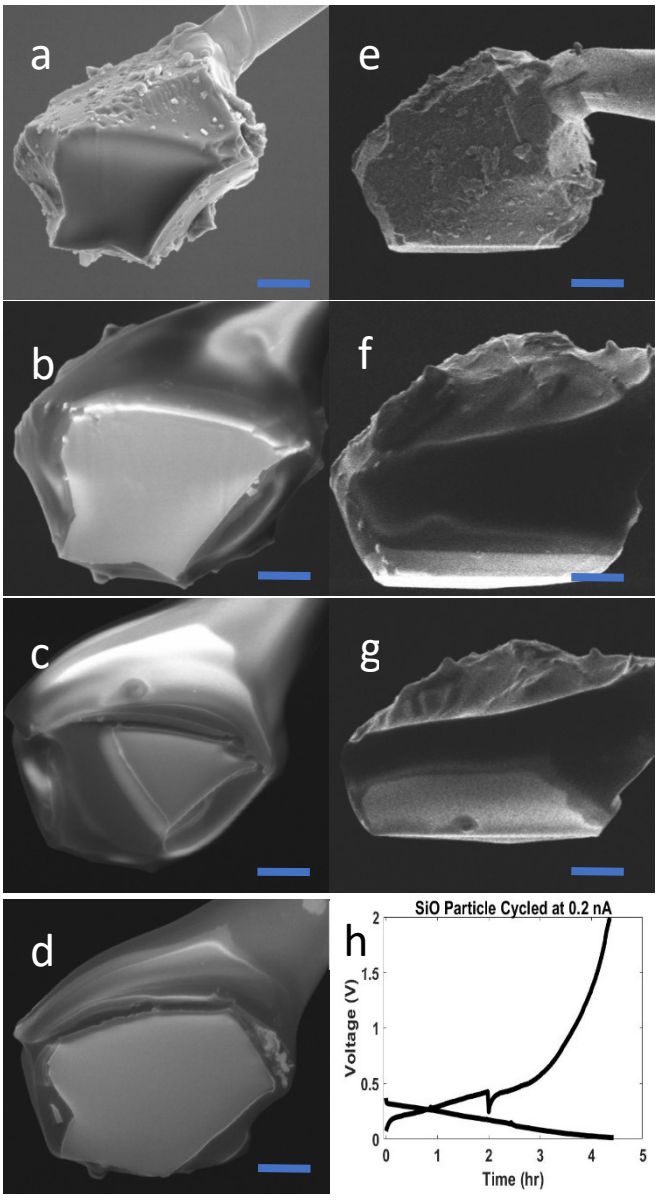

Figure 4 Front and top view of SiO particle were taken by SEM (left column) and FIB (right column), respectively, at various states of lithiation: (a/e) before lithiation, (b/f) after full

lithiation, (c/g) after full delithiation, and (d) cross section of fully delithiated SiO, (h) voltage profile of lithiation and delithiation with constant current at 0.2 nA. The scale bar in (a)-(g) is 2 μm.

After complete lithiation, the front and top views of the further polished SiO particle are shown in **Figure 4b** and **Figure 4f**. The fully lithiated SiO particle size apparently became much larger compared to its pristine state. However, the volume expansion of fully lithiated SiO is much smaller than that of the lithiated pure Si. In addition, the overall shape of SiO is almost kept the same without any irregular features as seen for the lithiated Si particle. When looking at the polished front side, the surface is very smooth, and no cracks are observed. Furthermore, the front contour line of the lithiated particle after polishing is enlarged, compared to that of the pristine SiO, but kept the same shape, suggesting that the volume expansion of SiO particle is isotropic. Before full lithiation, the lithiation of SPB was interrupted at 50% state of charge. The FIB and SEM images were taken, as shown in **Figure S1a** and **Figure S1b**, are similar to the fully lithiated SiO particle with less volume expansion.

The delithiated SiO particle is shown in **Figure 4c** and **Figure 4g**. Compared to its fully lithiated state, the delithiated SiO particle shrinks, but does not go back to the original size of the pristine SiO particle. The overall shape of SiO remains almost the same as the pristine particle. When looking at the polished front side, the surface is still very smooth without observable cracks. The front contour line of the delithiated particle in Figure 3c has changed, compared to that of the pristine and fully lithiated SiO, which is due to mis-cut. The original contour line appears after more than 20 times of repeated polishing, as shown in **Figure 4d**. In this figure, the front surface

is over 100 nm deep and represents the internal microstructure of the bulk SiO particle. Therefore, regardless of state of charge, pristine, partial lithiation, full lithiation, partial delithiation (shown in **Figure S2a** and **Figure S2b**), and full delithiation, very smooth and crack-free microstructure was observed for this 10 μm size SiO particle. The more detailed microstructure of the fully delithiated SiO particle during the polishing process can be seen in the supporting movie-SiO.

According to the SPB investigation on Si and SiO particles, it is not surprising to observe the particle fracture of the Si particle when it was charged and discharged, as in real batteries without any constraint. However, the fracture behavior of Si cannot be solely attributed to its large volume expansion (300%). We believe that the nonuniform volume expansion, crack and pore/concave formation of Si particles are also related to the lithiation kinetics, which are controlled by the migration of the interface. [25-28] Therefore, the lithiation occurs through a ledge mechanism involving the lateral movement of ledges on the close-packed (111) atomic planes leading to the orientation-dependent mobility of the interfaces and anisotropic swelling. As for the SiO particle, the Si domains in the SiO particle are only a few nanometers, as shown in **Figure 2c** and consistent to previous report on SiO [29]. SiO_x adjacent to Si domains will react with Li to form Si and Li_2O first. Li_2O is a good lithium conductor. The nano sized Si will be enclosed by Li_2O network and reacts with Li to form Li_xSi alloys with volume expansion. The Li_2O phase will buffer the volume change of nano sized Si. This microstructure makes the whole volume expansion of the micro sized SiO particle isotropic. In addition, the Si nano domains are too small to observe the orientation-dependent mobility. The very localized anisotropic swelling, if any, can be further mitigated by the uniformly distributed SiO_2 domains around the Si nano

domains. Overall, the micrometer size SiO particle appears to experience isotropic swelling, which leads to reversible expansion and contraction during lithiation and delithiation and a crack-free microstructure.

CONCLUSION

The single Si and SiO particle batteries were fabricated in FIB/SEM and successfully charged and discharged galvanostatically as in real batteries. The in-situ microstructure changes of Si and SiO particles were observed from two different angles using ion and electron beams at both lithiated and delithiated states. The volume expansion of free-standing micrometer size Si particle appears to be anisotropic with cracks and pores after only one cycle. However, the micrometer size SiO particle shows much less volume expansion. Most importantly, the volume expansion of the SiO particle is uniform and no cracks were observed from the inside to the outside, which can reduce the parasitic reaction between the electrolyte and SiO particle and increase the cycle life of LIB.

ASSOCIATED CONTENT

Supporting Information

Experimental method including single particle battery (SPB) fabrication; electrochemical charge and discharge; Focus Ion Beam (FIB) and Scanning Electron Microscopy (SEM). Movies during FIB for both Si and SiO particles. Supporting figures for SiO images in the middle of state of charge (SOC) during both lithiation and delithiation.

AUTHOR INFORMATION

Corresponding author

Wenquan Lu, Chemical Sciences and Engineering, Argonne National Laboratory, Lemont IL 60439, https://orcid.org/0000-0001-8655-8256, email: luw@anl.gov

Authors

Xinwei Zhou, Center for Nanomaterials, Argonne National Laboratory, Lemont, IL 60439; and Department of Mechanical and Energy Engineering, Indiana University Purdue University Indianapolis, Indianapolis, IN 46202

Yuzi Liu, Center for Nanomaterials, Argonne National Laboratory, Lemont, IL 60439

Likun Zhu, Department of Mechanical and Energy Engineering, Indiana University Purdue University Indianapolis, Indianapolis, IN 46202, https://orcid.org/0000-0002-6324-3718

Notes

The authors declare no competing financial interest.

ACKNOWLEDGMENTS

The authors gratefully acknowledge the support from the U.S. Department of Energy, Vehicle Technologies Office. This work was performed, in part, at the Center for Nanoscale Materials and Advanced Photon Sources, U.S. Department of Energy Office of Science User Facilities, and supported by the U.S. Department of Energy, Office of Science, under Contract No. DE-AC02-06CH11357.

REFERENCES

1. Kasavajjula, U.; Wang, C. S.; Appleby, A. J., Nano- and Bulk-Silicon-Based Insertion Anodes for Lithium-Ion Secondary Cells. *Journal of Power Sources* **2007,** *163* (2), 1003-1039.

2. Wu, H.; Cui, Y., Designing Nanostructured Si Anodes for High Energy Lithium Ion Batteries. *Nano Today* **2012,** *7* (5), 414-429.

3. Obrovac, M. N.; Christensen, L., Structural Changes in Silicon Anodes During Lithium Insertion/Extraction. *Electrochemical and Solid State Letters* **2004,** *7* (5), A93-A96.

4. Chan, C. K.; Peng, H. L.; Liu, G.; McIlwrath, K.; Zhang, X. F.; Huggins, R. A.; Cui, Y., High-Performance Lithium Battery Anodes Using Silicon Nanowires. *Nature Nanotechnology* **2008,** *3* (1), 31-35.

5. Scrosati, B.; Hassoun, J.; Sun, Y. K., Lithium-Ion Batteries. A Look into the Future. *Energy & Environmental Science* **2011,** *4* (9), 3287-3295.

6. Szczech, J. R.; Jin, S., Nanostructured Silicon for High Capacity Lithium Battery Anodes. *Energy & Environmental Science* **2011,** *4* (1), 56-72.

7. Yang, Y.; Yuan, W.; Kang, W. Q.; Ye, Y. T.; Pan, Q. Q.; Zhang, X. Q.; Ke, Y. Z.; Wang, C.; Qiu, Z. Q.; Tang, Y., A Review on Silicon Nanowire-Based Anodes for Next-Generation High-Performance Lithium-Ion Batteries from a Material-Based Perspective. *Sustainable Energy & Fuels* **2020,** *4* (4), 1577-1594.

8. Sun, Y. M.; Liu, N. A.; Cui, Y., Promises and Challenges of Nanomaterials for Lithium-Based Rechargeable Batteries. *Nature Energy* **2016,** *1*, 10671

9. Liu, X.; Du, Y.; Hu, L.; Zhou, X.; Li, Y.; Dai, Z.; Bao, J., Understanding the Effect of Different Polymeric Surfactants on Enhancing the Silicon/Reduced Graphene Oxide Anode Performance. *The Journal of Physical Chemistry C* **2015,** *119* (11), 5848-5854.

10. Zhou, X.; Ge, X.; Liu, S.; Qiao, M.; Du, Y.; Li, Y.; Bao, J., Enabling Superior Electrochemical Properties for Highly Efficient Potassium Storage by Impregnating Ultrafine Sb Nanocrystals within Nanochannel-Containing Carbon Nanofibers. *Angewandte Chemie International Edition* **2019,** *58, 14578*.

11. Zhang, L.; Deng, J. W.; Liu, L. F.; Si, W. P.; Oswald, S.; Xi, L. X.; Kundu, M.; Ma, G. Z.; Gemming, T.; Baunack, S.; Ding, F.; Yan, C. L.; Schmidt, O. G., Hierarchically Designed SiO_x/SiO_y Bilayer Nanomembranes as Stable Anodes for Lithium Ion Batteries. *Advanced Materials* **2014,** *26* (26), 4527-4532.

12. Park, C. M.; Choi, W.; Hwa, Y.; Kim, J. H.; Jeong, G.; Sohn, H. J., Characterizations and Electrochemical Behaviors of Disproportionated SiO and Its Composite for Rechargeable Li-Ion Batteries. *Journal of Materials Chemistry* **2010,** *20* (23), 4854-4860.

13. Miyachi, M.; Yamamoto, H.; Kawai, H.; Ohta, T.; Shirakata, M., Analysis of SiO Anodes for Lithium-Ion Batteries. *Journal of the Electrochemical Society* **2005,** *152* (10), A2089-A2091.

14. Kim, T.; Park, S.; Oh, S. M., Solid-State Nmr and Electrochemical Dilatometry Study on Li^+ Uptake/Extraction Mechanism in Sio Electrode. *Journal of the Electrochemical Society* **2007,** *154* (12), A1112-A1117.

15. Kim, J. H.; Sohn, H. J.; Kim, H.; Jeong, G.; Choi, W., Enhanced Cycle Performance of SiO-C Composite Anode for Lithium-Ion Batteries. *Journal of Power Sources* **2007,** *170* (2), 456-459.

16. Kim, H. J.; Choi, S.; Lee, S. J.; Seo, M. W.; Lee, J. G.; Deniz, E.; Lee, Y. J.; Kim, E. K.; Choi, J. W., Controlled Prelithiation of Silicon Monoxide for High Performance Lithium-Ion Rechargeable Full Cells. *Nano Letters* **2016,** *16* (1), 282-288.

17. Hwa, Y.; Park, C. M.; Sohn, H. J., Modified SiO as a High Performance Anode for Li-Ion Batteries. *Journal of Power Sources* **2013,** *222*, 129-134.

18. Yan, M.-Y.; Li, G.; Zhang, J.; Tian, Y.-F.; Yin, Y.-X.; Zhang, C.-J.; Jiang, K.-C.; Xu, Q.; Li, H.-L.; Guo, Y.-G., Enabling SiO_x/C Anode with High Initial Coulombic Efficiency through a Chemical Pre-Lithiation Strategy for High-Energy-Density Lithium-Ion Batteries. *ACS Applied Materials & Interfaces* **2020,** *12* (24), 27202-27209.

19. Mamiya, M.; Takei, H.; Kikuchi, M.; Uyeda, C., Preparation of Fine Silicon Particles from Amorphous Silicon Monoxide by the Disproportionation Reaction. *Journal of Crystal Growth* **2001,** *229* (1), 457-461.

20. Chen, T.; Hu, J. Z.; Zhang, L.; Pan, J.; Liu, Y. Y.; Cheng, Y. T., High Performance Binder-Free SiO_x/C Composite Lib Electrode Made of Siox and Lignin. *Journal of Power Sources* **2017,** *362*, 236-242.

21. Zhou, X.; Li, T.; Cui, Y.; Fu, Y.; Liu, Y.; Zhu, L., In Situ Focused Ion Beam Scanning Electron Microscope Study of Microstructural Evolution of Single Tin Particle Anode for Li-Ion Batteries. *ACS Applied Materials & Interfaces* **2019,** *11* (2), 1733-1738.

22. Zhou, X. W.; Li, T. Y.; Cui, Y.; Meyerson, M. L.; Mullins, C. B.; Liu, Y. Z.; Zhu, L. K., In Situ Focused Ion Beam-Scanning Electron Microscope Study of Crack and Nanopore Formation in Germanium Particle During (De)Lithiation. *Acs Applied Energy Materials* **2019,** *2* (4), 2441-2446.

23. Xiong, B. Q.; Zhou, X. W.; Xu, G. L.; Liu, Y. Z.; Zhu, L. K.; Hu, Y. C.; Shen, S. Y.; Hong, Y. H.; Wan, S. C.; Liu, X. C.; Liu, X.; Chen, S. L.; Huang, L.; Sun, S. G.; Amine, K.; Ke, F. S., Boosting Superior Lithium Storage Performance of Alloy-Based Anode Materials Via Ultraconformal Sb Coating-Derived Favorable Solid-Electrolyte Interphase. *Advanced Energy Materials* **2020,** *10* (4), 1903186.

24. Amine, R.; Daali, A.; Zhou, X.; Liu, X.; Liu, Y.; Ren, Y.; Zhang, X.; Zhu, L.; Al-Hallaj, S.; Chen, Z.; Xu, G.-L.; Amine, K., A Practical Phosphorus-Based Anode Material for High-Energy Lithium-Ion Batteries. *Nano Energy* **2020,** *74*, 104849.

25. Liu, X. H.; Wang, J. W.; Huang, S.; Fan, F. F.; Huang, X.; Liu, Y.; Krylyuk, S.; Yoo, J.; Dayeh, S. A.; Davydov, A. V.; Mao, S. X.; Picraux, S. T.; Zhang, S. L.; Li, J.; Zhu, T.; Huang, J. Y., In Situ Atomic-Scale Imaging of Electrochemical Lithiation in Silicon. *Nature Nanotechnology* **2012,** *7* (11), 749-756.

26. Goldman, J. L.; Long, B. R.; Gewirth, A. A.; Nuzzo, R. G., Strain Anisotropies and Self-Limiting Capacities in Single-Crystalline 3d Silicon Microstructures: Models for High Energy Density Lithium-Ion Battery Anodes. *Advanced Functional Materials* **2011,** *21* (13), 2412-2422.

27. Pharr, M.; Zhao, K.; Wang, X.; Suo, Z.; Vlassak, J. J., Kinetics of Initial Lithiation of Crystalline Silicon Electrodes of Lithium-Ion Batteries. *Nano Letters* **2012,** *12* (9), 5039-5047.

28. Shi, F.; Song, Z.; Ross, P. N.; Somorjai, G. A.; Ritchie, R. O.; Komvopoulos, K., Failure Mechanisms of Single-Crystal Silicon Electrodes in Lithium-Ion Batteries. *Nature Communications* **2016,** *7* (1), 11886.

29. Hirata, A.; Kohara, S.; Asada, T.; Arao, M.; Yogi, C.; Imai, H.; Tan, Y.; Fujita, T.; Chen, M., Atomic-Scale Disproportionation in Amorphous Silicon Monoxide. *Nature Communications* **2016,** *7* (1), 11591.